Interdependence between Structural Engineering and Construction Management
Edited by Ozevin, D., Ataei, H., Modares, M., Gurgun, A., Yazdani, S., and Singh, A.

ISBN: 978-0-9960437-6-2

SEISMIC EVALUATION OF SQUARE HSS BRACES IN SCBF USING REGRESSION ANALYSIS

MAHMOUD FAYTAROUNI[1], ONUR SEKER[2], BULENT AKBAS[3], and JAY SHEN[1]

[1]*Dept of Civil, Construction and Environmental Engineering, Iowa State University, Ames, USA*
[2]*Dept of Civil Engineering, MEF University, Istanbul, Turkey*
[3]*Dept of Civil Engineering, Gebze Technical University, Kocaeli, Turkey*

Since the 1990s, structural engineering practice geared toward the use of hollow structural sections (HSS), notably square HSS, for their economy, and ease of design and construction. According to the AISC Seismic Provisions, during a severe earthquake, these braces could undergo post-buckling axial deformations 10 to 20 times their yielding deformation. However, recent experimental studies indicate that braces made of square HSS, depending on their size, width-to-thickness, and slenderness ratio, are vulnerable to fracture even prior to 10. Therefore, relying on past experimental studies comprised of a few square HSS specimens to develop seismic requirements for SCBF with square HSS could lead to underestimation of the seismic risk. This paper aims to evaluate the fracture risk of braces in existing SCBFs designed in accordance with AISC 341-05 and AISC 341-16 through incremental dynamic analyses (IDA) along with experimentally developed regression model that estimates fracture.

Keywords: Seismic risk, Incremental dynamic analysis, Ductility capacity and demand, Fracture.

1 INTRODUCTION

The seismic design criteria adopted in the design codes for special concentrically braced frames (SCBFs) is tailored based on the concept of capacity design. In the design procedure of SCBFs, plastic deformations are confined to braces only, leaving other structural members such as beams and columns to remain elastic. According to the commentaries in AISC 341-05 (2005) and AISC 341-16 (2016): During a severe earthquake, braces in SCBF could undergo post-buckling axial deformations 10 to 20 times their yield deformation. This ductility demand range is based on the experimental and analytical work conducted by Goel (1992). The experimental portion of the study included braces varying between large- and small-size sections of various shapes such as wide flanges, angles, and tubes. However, since 1990s engineering practice geared toward the use of hollow structural sections (HSS), notably square HSS, for their ease of design and construction. Numerous experimental studies have been conducted on conventional bracings made of square HSS over the last decades. The results of these tests indicate that braces with square HSS are vulnerable to fracture even prior to 10, the lower bound of the expected ductility demand (Goel 1992).

In this study, experimental cyclic tests on square HSS braces conducted from 1978 to 2013 have been thoroughly surveyed. A total of 79 square HSS braces were collected from 16 experimental programs. For each specimen, the ductility capacity reached fracture was

estimated and reported. Collected specimens with sizes of HSS 5x5 and HSS 6x6 reached a mean ductility capacity of 9.0, while with a larger size of HSS 10x10, the possessed ductility capacity at fracture was 8.0. This experimental observation agrees with the analytical findings of Shen *et al.* (2017). Their study concludes that braces in SCBF are often likely to fracture prior to the expected story drift ratio (SDR) demand. Therefore, relying on past experimental results comprised of a few test results to develop seismic requirements for SCBF with square HSS could lead to brace fracture earlier than expected as well as underestimation of the overall seismic risk. The purpose of this paper is to evaluate the fracture risk of braces in existing SCBFs designed following AISC 341-05 (2005) and AISC 341-16 (2016) through incremental dynamic analyses (IDA) along with the experimentally developed regression model that estimates fracture life.

2 CASE STUDY BUILDINGS AND CALIBRATION

2.1 Building Description

The seven-story office buildings adopted in the NEHRP Recommended Seismic Provisions: Design Examples under publication number of FEMA P-751 (NEHRP 2012), and FEMA P-1051 (NEHRP 2016) were investigated in this study. The seven-story office building is located in Los Angeles, California. Figure 1(a) illustrates the plan dimensions of the building. The height of the first story, as shown in Figure 1(b), is 22 feet while all remaining stories are 13 feet in height. In Table 1, and throughout the paper, the SCBF designed in FEMA P-751 (NEHRP 2012) is identified as Frame A, whereas Frame B is given to that designed in FEMA P-1051 (NEHRP 2016). Note that the designs of Frames A and B are in compliance with AISC 341-05 (2005) and AISC 341-16 (2016), respectively. Detailed information on the design process and buildings can be found in (NEHRP 2012 and 2016).

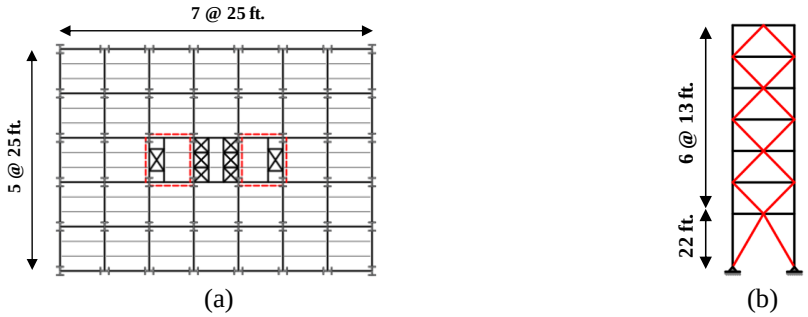

Figure 1. (a) floor plan view, and (b) elevation of the two-story X bracing configuration.

Table 1. Member sizes of the considered seven-story SCBFs.

Story Level	Frame A			Frame B		
	Braces	Columns	Beams	Braces	Columns	Beams
7	HSS 5 ½ ×5 ½×5/16	W 14×53	W 18×35	HSS 5×5×3/8	W 14×68	W 18×40
6	HSS 6×6×1/2	W 14×61	W 18×35	HSS 6×6×1/2	W 14×159	W 18×50
5	HSS 6×6×5/8	W 14×61	W 18×35	HSS 7×7×1/2	W 14×159	W 18×50
4	HSS 6×6×5/8	W 14×132	W 18×35	HSS 7×7×1/2	W 14×342	W 18×60
3	HSS 7×7×1/2	W 14×132	W 18×35	HSS 7×7×1/2	W 14×342	W 18×40
2	HSS 8×8×5/8	W 14×233	W 18×35	HSS 8×8×1/2	W 14×550	W 18×65
1	HSS 9×9×5/8	W 14×233	W 27×102	HSS 9×9×5/8	W 14×550	W 30×132

2.2 Analytical Models of the Frames and Validation Study

Frames A and B were built as two-dimensional (2D) analytical models within *OpenSees* (McKenna *et al*. 2000). The modeling conditions were validated using the shaking table test of the nearly full-scale chevron CBF frame presented in (Okazaki *et al*. 2012). The one-story tested frame shown in Figure 2(a) comprised of braces and columns with square HSS sections, whereas the beam section was a built-up wide-flange. The unit of the sections presented in Figure 2(a) is inches. The frame was subjected to a series of ground shaking using the same ground motion with different intensities. The focus herein is on the experimental results of the overall frame and brace response at 42% motion.

First, a fundamental period of T_1=0.20 seconds was determined from the eigenvalue analysis, which was closely matching to T_1 of the test (Okazaki *et al*. 2012). Accordingly, the frame was subjected to the ground shaking time history measured during the test. Figure 2 compares the analytical and experimental time history response of the frame in terms of lateral displacement and the east side brace's hysteresis. As Figures 2(b) and (c) illustrate, a good agreement was observed from both the displacement time history and brace response under the motion. One can notice that the main characteristics of this dynamic test were captured quite well, and thus the analytical models (i.e., Frames A and B) deemed to be sufficiently reliable for analyzing the frames under several ground motions.

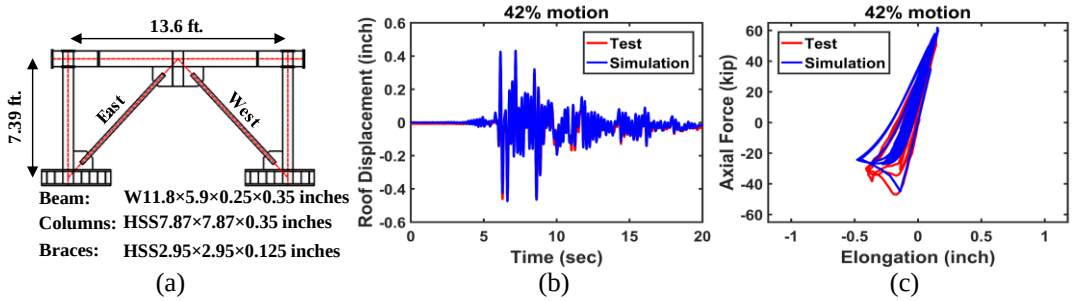

Figure 2. Comparison of the simulated and the experimental responses under 42% motion: (a) tested frame by Okazaki *et al.* (2012), (b) roof displacement time history, (c) brace response.

3 DUCTILITY-BASED REGRESSION MODEL FOR EVALUATING SQUARE HSS

Braces designed in accordance with AISC 341-05 (2005) and AISC 341-16 (2016) are required to satisfy the limits on width-to-thickness (b/t) and slenderness (KL/r) ratios. These seismic limits are set to achieve adequate ductility on the order of 10 to 20 without experiencing fracture. However, the comprehensive survey of the experimental cyclic tests on square HSS, reported in Figure 3, indicates that fracture for specimens designed to satisfy b/t and KL/r is more likely to occur within the expected ductility demand range (10-20). The collected specimens included 79 square HSS braces from 16 experimental programs. For each specimen, the ductility capacity at fracture (μ_c) was estimated from the published plots. Note that both ductility capacity (μ_c) and demand (μ_d) are defined as the axial brace deformation in either tension or compression, whichever is larger, normalized by yielding or buckling deformation. Figure 3(a), (b), and (c) report the interaction between μ_c and b/t, KL/r, and the material parameters (E/F_y), where E is elastic modulus, and F_y is yielding strength. Referring to Figure 3, one might observe the following: (a) majority of the tested specimens that satisfy b/t and KL/r ratios stipulated in AISC 341-05 (2005) and AISC 341-16 (2016) experienced fracture

prior to attaining a ductility capacity of 20 and 15, respectively, and (b) although μ_c appeared to be inversely proportional to b/t and directly proportional to the ratio of KL/r and E/Fy to a certain degree, an apparent trend is lacking due to the robust interaction between these parameters.

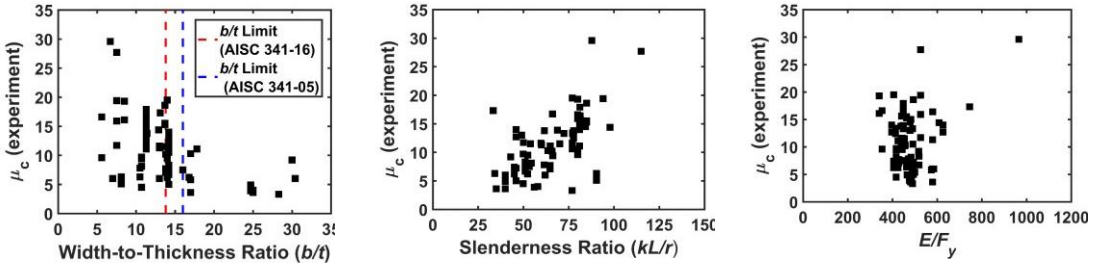

(a) (b) (c)

Figure 3. Ductility capacity of the collected 79 specimens at fracture: (a) interaction between ductility capacity at fracture (μ_C) and width-to-thickness ratio (b/t), (b) interaction between μ_C and slenderness ratio (KL/r), and (c) interaction between μ_C with the mechanical properties (E/F_y).

3.1 Regression Analysis

Multiple nonlinear regression analyses were performed on the collected data (Figure 3) to attain a relationship between ductility capacity at fracture (μ_c) and the geometric- material parameters (i.e., b/t, KL/r, and E/F_y). The regression effect summary has shown that the combined interaction between the multiple predictors such as b/t, KL/r, and E/F_y all have a profound impact and play an essential role in determining μ_c at fracture. Consequently, and after several regression iterations, two polynomial equations to the 5th degree were found to be adequate to estimate μ_c at fracture for the specimens satisfying limiting b/t and KL/r ratios specified in AISC 341-05 (2005) and AISC 341-16 (2016). It is noteworthy that the estimation addressed in Eq. (1) is only applicable to the specimens that satisfy AISC 341-05 (2005) limits, whereas Eq. (2) is driven for those satisfying AISC 341-16 (2016). Table 2 summarizes the coefficients that offer the optimal fit. The statistical measure of the predictive model fit adjusted-R^2 of 0.6 and 0.68 for Eqs. (1) and (2), respectively. Accordingly, these equations are utilized to estimate the ductility capacity at fracture for the braces in Frames A and B.

Table 2. Regression coefficients in Eq. (1) and Eq. (2).

	Eq. (1)				Eq. (2)			
C(n)	2	3	4	5	2	3	4	5
C_1	-5.32E-01	-1.40E-01	1.71E-02	4.05E-03	-1.57E+00	-1.08E+00	1.49E-01	5.15E-02
C_2	-1.44E-03	-4.14E-04	-1.91E-06	2.58E-07	3.66E-03	-8.96E-05	-5.78E-07	9.71E-08
C_3	2.15E-05	-1.70E-06	1.16E-08	-1.66E-11	-4.35E-04	-5.65E-06	4.17E-08	-5.85E-11

$$\mu_c = -26.84 + 1.048b/t + 0.241KL/r - 0.023E\Big/F_y + \sum_{n=2}^{5} C_1(n)x(b/t - 11.78)^n + \cdots$$
$$C_2(n)x(KL/r - 67.43)^n + C_3(n)x(E/F_v - 475.85)^n \quad (1)$$

$$\mu_c = -95.62 + 6.484b/t + 0.159KL/r + 0.055E/F_y + \sum_{n=2}^{5} C_1(n)x(b/t - 10.7)^n + \cdots$$
$$C_2(n)x(KL/r - 72.68)^n + C_3(n)x(E/F_y - 474.86)^n \quad (2)$$

4 DUCTILITY DEMAND ON BRACES UNDER SELECTED GROUND MOTIONS

4.1 Selected Ground Motion Records

The seismic demand on the braces in Frames A and B was investigated using five ground motion (GM) records. The GM records were selected from the Pacific Earthquake Engineering Research (PEER) Center database (PEER 2018). The records were scaled, as presented in Figure 4, so that the geometric mean of the 5% damping response spectra of the scaled suite of ground motions is not lower than the target response spectrum over a period range. Note that the analytical first modal periods, T_1, were 1.07 seconds for Frame A and 0.94 seconds for Frame B.

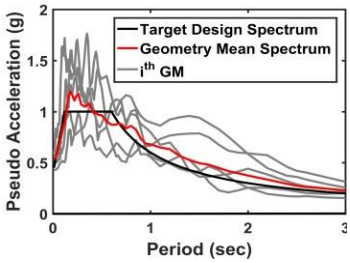

Figure 4. Response spectra of the ground motions used for IDA.

4.2 IDA Results and Conclusions

Incremental dynamic analysis (IDA) was carried out, where frames were subjected to a series of nonlinear dynamic analyses using records of increasing intensities. Once the IDA curves were established, the time history analyses, during which one of the seven stories undergo an SDR of 2% or 4%, were selected first. The ground shaking intensities corresponding to these response quantities are considered to represent the design level and collapse prevention level earthquakes, respectively. Subsequently, for the selected data points on each IDA curve, hysteretic loops of the braces are plotted. Then, the distribution of peak ductility demand (μ_d) on each brace along the height is investigated. In order for the discussions on the seismic risk assessment to be pertinent, the demand is required to be paired with its counterpart. Therefore, fracture life (i.e., ductility capacity) of each brace section used in the design was also estimated by means of the previously derived equations (i.e., Eqs. (1)- (2)) based on the inclusive collection of test data.

Figure 5 presents the estimated ductility capacity (μ_c) established with the *b/t*, *KL/r* and *E/Fy* of the braces along with the peak ductility demand (μ_d) on them. Blue and green solid lines in Figure 5 depict the median ductility demands as reliable response indicators when the frames are subjected to an SDR of 2% or 4%, respectively, while red solid line shows the estimated ductility capacity for each brace section. Note that peak μ_d represents the maximum ductility demand attained by any of the two braces located in each story level at any time step during the selected time history analysis.

One can observe from Figure 5 that peak ductility demand (μ_d) distribution of the two frames over ten GMs indicate that the braces located at the first story level attain the highest ductility demand among other stories. This concentration seems to result in significant demand reduction over higher stories. For example, a noticeable variation can be seen between the first two stories, where the peak μ_d of the braces is abruptly reduced almost by half from the first to second story. Further, the peak μ_d obtained from the first stories in both Frames A and B are within 10 and 20 at SDR of 2%, which is the ductility demand range that braces in SCBFs are expected to achieve without fracture at design level earthquakes according to AISC Seismic (AISC 341 2005, 2016). It is also notable that the ductility-based fracture life (i.e., μ_c) estimation by regression analysis indicates that likelihood of fracture for the braces other than the first story braces is quite low at 2% SDR for both frames. The first story braces, however, might experience fracture even at 2% SDR, since the demand exceeded the estimated capacity under some of the ground motions. As indicated in the green line in Figure 5, the median demand on the first story braces is about 28 and 31 in Frames A and B, respectively, when the frames were pushed further until an SDR of 4%. Comparing the estimated capacity and the demand shows that the first story brace in Frame A and the first three stories in Frame B were susceptible to fracture. Considering the number of GM records adopted in this study, further analysis is required to duly quantify and evaluate square HSS' vulnerability to fracture and its impact on seismic risk.

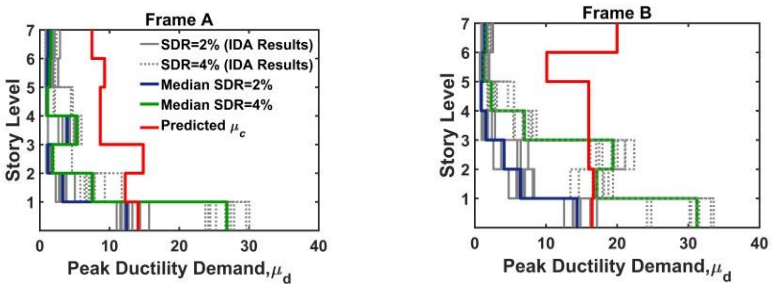

(a) (b)

Figure 5. Peak ductility demand (μ_d) distribution of braces along the building height obtained from IDA of the selected ground motions at story drift ratios (SDR) of 2% and 4%: (a) Frame A, (b) Frame B.

References

AISC 341-05, *Seismic Provisions for Structural Steel Buildings*, ANSI/AISC, Chicago, IL, American Institute of Steel Construction, 2005

AISC 341-16, *Seismic Provisions for Structural Steel Buildings*, ANSI/AISC, Chicago, IL, American Institute of Steel Construction, 2016.

Goel, S. C., Cyclic Post Buckling Behavior of Steel Bracing Members, *Stability and Ductility of Steel Structures Under Cyclic Loading*, Boca Raton, FL: CRC Press, 75-104, 1992.

McKenna, F., Fenves, G. L., and Scott, M. H., Open system for earthquake engineering simulation, *University of California, Berkeley, CA*, 2000.

NEHRP, Recommended Seismic Provisions: Design Examples: FEMA P-751, 2012.

NEHRP, Recommended Seismic Provisions: Design Examples: FEMA P-1051, 2016.

Okazaki, T., Lignos, D. G., Hikino, T., and Kajiwara, K., Dynamic Response of a Chevron Concentrically Braced Frame, *Journal of Structural Engineering*, *139*(4), 515-525, 2012.

Pacific Earthquake Engineering Research Center, 325 Davis Hall, University of California, Berkeley, CA 94720, 2018.

Shen, J., Seker, O., Akbas, B., Seker, P., Momenzadeh, S., and Faytarouni, M., 2017. Seismic performance of concentrically braced frames with and without brace buckling. *Engineering Structures*, *141*, 2017.